

Preliminary Analytical Approach to a Brachiation Robot Controller

Jun Nakanishi* and Toshio Fukuda

Department of Mechano-Informatics and Systems

Nagoya University

Nagoya, Aichi 464-01, Japan

Daniel E. Koditschek †

Department of Electrical Engineering and Computer Science

The University of Michigan

Ann Arbor, MI 48109-2110, USA

The University of Michigan EECS Department

Systems Division Technical Report: CGR 96-08

Computer Science and Engineering Division Technical Report: CSE TR 305-96

August, 1996

Abstract

We report on our preliminary studies of a new controller for a two-link brachiating robot. Motivated by the pendulum-like motion of an ape's brachiation, we encode this task as the output of a "target dynamical system." Numerical simulations indicate that the resulting controller solves a number of brachiation problems that we term the "ladder", "swing up" and "rope" problems. Preliminary analysis provides some explanation for this success. We discuss a number of formal questions whose answers will be required to gain a full understanding of the strengths and weaknesses of this approach.

1 Introduction

This paper presents our preliminary efforts to develop a new controller for a two degree of freedom brachiating robot. A brachiating robot dynamically moves from handhold to handhold like a long armed ape swinging its arms as depicted in Figure 1. This study considers a simplified two-link point mass lossless model with one actuator at the elbow connecting two arms, each of which has a gripper (see Figure 2). Clearly, this is an underactuated machine, having fewer actuators than its degrees of freedom. Thus, despite its relatively simple structure, designing a brachiating controller for such a system is challenging since the theory of underactuated mechanisms is not well established. In this paper we propose a new control scheme for the robot of Figure 2 and present some preliminary numerical studies of its properties.

A growing number of robotics researchers have taken an interest in building dynamically dexterous robots—machines that are required to interact dynamically with an otherwise unactuated

*The first author was at the Department of Electrical Engineering and Computer Science, the University of Michigan from September, 1995 to August, 1996.

†This work was supported in part by the US National Science Foundation under grant IRI-9510673.

environment [5] in order to achieve a designated task. Brachiating robots take an interesting place within this larger category of machines that juggle, bat, catch, hop and walk in the effort to achieve dynamically dexterous behavior analogous to that of humans and animals, for a brachiating and a legged locomotion system share the requirement of an oscillatory exchange of kinetic energy and potential energy in the gravitational field. At the same time, the problem of dexterous grasps is particularly acute for such machines since fumbles not only fail the task but incur a potentially disastrous fall as well. In this paper we confine our attention to a very simplified version of the former problem. In the long run, we suspect that the brachiation task may lend significant insight into general locomotion systems as well as still wider problems requiring dynamically dexterous hand-eye coordination.

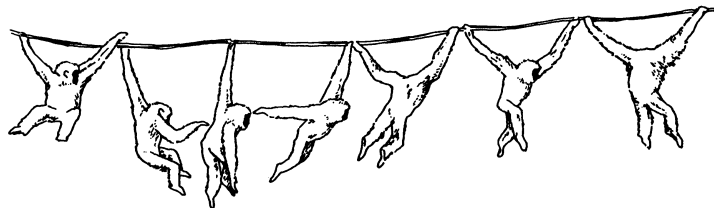


Figure 1: Brachiation of a gibbon: a picture taken from [13]

1.1 Problem Statement

Brachiation—arboreal locomotion via arms swinging hand over hand through the trees—is a form of locomotion unique to apes. Most commonly, the animals engage in “slow brachiation,” travelling at about the speed of the average human walk (slow brachiation). But when excited or frightened, apes can plunge through the forest canopy at astonishing speeds, sometimes covering 30 feet or more in a single jump without a break in “stride” (fast brachiation, ricocheting)[4]. In our reading of the biomechanics literature we distinguish three variants of brachiation that we will refer to in this paper as the

- Ladder and swing up problem
- Rope problem
- Leap problem

The first arises when an ape transfers from one branch to another and controlling the arm position at next capture represents the central task requirement. A robotics version of this problem has been previously introduced to the literature by the second author and colleagues [16, 17]. They presented the machine we model here with a set of discrete evenly spaced bars and the requirement to swing up from rest, catch the next bar, and then swing from bar to bar by pumping up energy in a suitable fashion. In our view, this problem seems as much akin to that of throwing and catching as to locomotion. In order to address the second problem that forms the chief interest of this paper, we find it useful to revisit this swing up and ladder problem along the way.

The third problem arises in the context of fast brachiation where the next branch is far out of reach and the task cannot be accomplished without a large initial velocity and a significant component of free flight. Solving this problem involves not merely a swing phase but a nonholonomic flight as well. Roughly analogous to running quickly through a field of boulders, apes can apparently

achieve this movement with great regularity and ease. We consider this a fascinating and challenging problem to be addressed when the previous two simpler problems are better understood.

In this paper we are centrally concerned with the second problem: brachiation along a continuum of handholds—a branch or a rope—that seems most closely analogous to human walking. Since grasps are afforded at will, the resulting freedom of placement can be exploited to achieve a specified forward rate of progress. This is not possible for a two degree of freedom machine on a ladder whose forward velocity is essentially determined by the distance between the bars and its own kinematics. We propose a control algorithm which is effective for the first two “slow brachiation” problems—i.e. the ladder and swing up and rope problems—inspired by our reading of the biomechanics literature. Specifically, Preuschoft *et al.* [8] studied the mechanics of ape brachiation and identified a close correspondence between slow brachiation and the motion of a simplified pendulum. Accordingly, we have chosen formally to encode the problem of slow brachiation in terms of the output of a target dynamical system—the harmonic oscillator—and this task specification lends a slightly new twist to the traditional view of underactuated mechanisms, as we now discuss.

1.2 Related work

As we have pointed out, this problem domain overlaps with three areas of robotics: dexterous manipulation, legged locomotion and underactuated mechanisms. We now review the relationship of our ideas and contributions to this previous literature.

Problems of dexterous manipulation have given rise to a growing literature concerned with explicit manipulation of an environment’s kinetic as well as potential energy. Arguably, the first great success in this domain must be attributed to Andersson [1] whose ping pong playing robot developed a decade ago was capable of beating many humans. Some of the earliest work in the area has also been undertaken by the third author and his students [2, 3, 10] who have developed a family of juggling robots that exhibit increasingly sophisticated strategic as well as mechanical skills in various “games against nature.” More recently, Mason and Lynch [7] have studied the problem of dynamic underactuated nonprehensile manipulation from the control theoretic point of view and have successfully implemented a family of formally designed control laws on a one degree of freedom robot which performs dynamic tasks such as snatching, rolling, throwing and catching. Of these antecedents, the present study is most reminiscent of the juggling work since our approach to control entails feedback regulation rather than the open loop pre-planned trajectories developed by Mason and Lynch or the AI system developed by Andersson.

Raibert’s landmark success in legged locomotion [9] represents another important influence on the present work. The third author and students have pursued a number of analytical studies of simple hopping machines that are directly inspired by his work addressing such questions as regulation of hopping height [6], forward velocity [11] and duty factor [12]. The formulation of this brachiation problem in terms of a target dynamics owes much to Raibert’s original notion that dynamical dexterity may be encoded in terms of desired energy and achieved with the help of the environment’s intrinsic dynamics. Moreover, we have adapted his use of a reverse time symmetry to our problem setting.

Amidst the large and growing controls literature on underactuated mechanisms, this work is closest in method to Spong and his students’ studies of the “Acrobot” [15]. They considered the swing up problem of an underactuated system similar to the two-link brachiating robot we treat in this paper. Their control algorithm pumps energy to the system in an instance of Spong’s more general notion of partial feedback linearization [14] directed toward achieving a kind of target dynamics whose motions solve the swing up problem. The controller we introduce here bears many similarities to this although the more extended problems of slow brachiation require a rather differently conceived notion of target dynamics.

Finally, we must mention the initial success in robot brachiation achieved by the second author and his student Saito [16]. They first studied the control problem of a two-link brachiating robot using a heuristic learning algorithm to formulate a control law. They also built a physical two-link brachiating robot and experimentally demonstrated the validity of the control law. The advantage of this method is that no model of a robot is needed. However, it requires a large number of trials and errors to generate a motion. Then they considered the control of a brachiating robot with higher degrees of freedom, and built the brachiating robot with 12 degrees of freedom modelled on a real long-armed ape. They succeeded as well in the basic experiment generating brachiation behavior of this robot using a manually tuned control strategy [17].

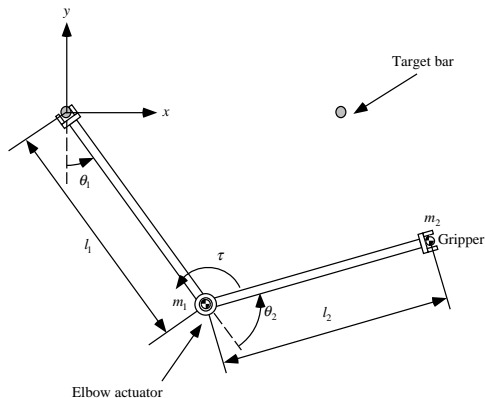


Figure 2: The model of a two-link brachiating robot

2 Task Encoding via Target Dynamics

This section presents our control strategy for a two-link brachiating robot. We view the robot’s task to be one of solving an “environmental control problem” [2]. For example, in robot juggling a fully actuated robot controls the motion of a ball (which is the unactuated environment) through intermittent interaction. In this case, interaction between the robot and environment only occurs at the ball-robot impact. In contrast, in robot brachiation, the robot and environment (respectively the actuated and unactuated joints) have continuous interaction during the motion. The difficulty in controlling a brachiating robot arises due to this continuous coupling. Hopping robots might be considered as lying in between since they have continuous interaction with the ground only in the stance phase.

Appropriate task encoding plays an important role in achieving robot dynamical dexterity in dynamical environment. Before proceeding, we mention some previous instances of task encoding based on a good understanding of the intrinsic dynamics of a system and an environment.

The first example of task encoding is in the control of legged locomotion by Raibert[9]. He decomposes the control of legged locomotion into three parts and encodes as:

- Regulation of hopping height: control of the mechanical energy of the system through leg’s thrust.
- Control of forward velocity: choice of foot placement at touchdown.
- Control of body posture: servoing the hip during stance.

He implements a simple feedback control law to achieve the desired locomotion according to this task encoding and successfully demonstrated the validity of his control strategy.

The second example is in the robot juggling achieved by the third author *et al.*[2]. Their idea is analogous to that of Raibert’s. In order to achieve juggling with the specific apex height of a ball they introduce a “mirror algorithm” by means of which the robot is forced to track the nonlinear reflected mirror trajectory of a ball servoing its mechanical energy around a desired steady state energy level. In these examples, appropriate task encoding achieves such dynamically dexterous behavior as hopping and juggling.

First we review the biomechanics of brachiation. Average horizontal velocity of brachiation is characterized in terms of the motion of a simplified pendulum, to which slow brachiation is analogous. We next introduce the notion of “target dynamics” as a particular instance of input/output plant inversion. Specifically, brachiation is encoded as the output of a target dynamical system—a harmonic oscillator, that we must force the robot to mimic.

2.1 Review of Biomechanics of Brachiation: A Target Dynamics

According to the biomechanics literature [8] slow brachiation of apes resembles the motion of a pendulum. Although the ape’s moment of inertia varies during the swing according its change of posture, the motion of a simplified pendulum gives a fairly good approximation. We briefly review the characterization of the forward velocity of brachiation using Figure 3 as suggested in [8].



Figure 3: A suspended body of an ape represented by a simplified pendulum. An ape’s body is approximated by a simple pendulum.

Consider the dynamics of a simple pendulum with a point mass and a massless link:

$$\ddot{\xi} = -\frac{g}{l_0} \sin \xi \quad (1)$$

where l is pendulum length and g is the gravitational constant.

The average horizontal velocity is the net progress per swing divided by half the period of oscillation. For a given initial angle α_0 , the period of oscillation is

$$T = 4K(k) \sqrt{\frac{l_0}{g}} \quad (2)$$

where $K(k) = \int_0^{\frac{\pi}{2}} \frac{d\phi}{\sqrt{1-k^2 \sin^2 \phi}}$ is a complete elliptic integral of the first kind and $k = \sin(\frac{\alpha_0}{2})$. The net progress covered by one swing is

$$d(\alpha_0) = 2l_0 \sin \alpha_0 \quad (3)$$

Thus, the average forward velocity of brachiation for a pendulum starting at $\xi(0) = \alpha_0$ is

$$\bar{h} = \frac{d(\alpha_0)}{2K(k(\alpha_0))} \sqrt{\frac{g}{l_0}} = \frac{\sqrt{gl_0} \sin \alpha_0}{K(k(\alpha_0))} := V_1(\alpha_0) \quad (4)$$

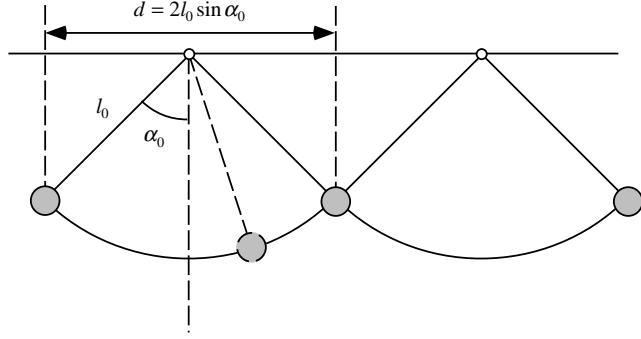


Figure 4: Brachiation represented by the motion of a simple pendulum. The average forward velocity is characterized by the ratio of the net progress per swing divided by the time needed.

We will approximate (1) by $\ddot{x} = -\omega^2 x$ to resulting in an approximation for (2) as

$$\hat{T} = \frac{2\pi}{\omega} \quad (5)$$

and (4) as

$$\hat{h} = \frac{d(\alpha_0)\omega}{\pi} = \frac{2l_0\omega \sin \alpha_0}{\pi} := \hat{V}_1(\alpha_0) \quad (6)$$

2.2 Approaches to Controlling Underactuated Systems

The notion of target dynamics represents a variant on standard techniques of plant inversion. A system is inverted then forced to have the characteristic of some target dynamics. The application of this idea to the two-link brachiating robot is presented.

2.2.1 Partial Linearization of Underactuated Lagrangian Systems

Let us generalize slightly Spong's notion of partial feedback linearization in [14] as follows.

Suppose a plant

$$\dot{w} = F(w, v) \quad (7)$$

$$y = H(w) \quad (8)$$

is input/output linearizable. That is, given

$$L_F H(w, v) = DH \cdot F(w, v) \quad (9)$$

if there can be found an implicit function such that for every $u \in \mathcal{U}$ and $w \in \mathcal{W}$, then

$$v = L_F H^{-1}(w, u) \quad (10)$$

implies

$$L_F H(w, v) = u \quad (11)$$

then (10) is an input/output linearizing inverse controller in the sense that $\dot{y} = u$.

For the case of the Lagrangian systems that concern us here, consider an n degree of freedom underactuated system with $m < n$ degrees of freedom directly driven by each actuator and $k = n - m$ unactuated degrees of freedom. Let $q \in \mathcal{Q}$ be the generalized coordinates and $Tq = [q, \dot{q}]^T \in T\mathcal{Q}$ be the associated tangent vector. The dynamics of such a system can be written as

$$\dot{T}q = \mathcal{L}(Tq, \tau) \quad (12)$$

where

$$\mathcal{L}(Tq, \tau) = \left[M(q)^{-1} \left(\begin{array}{c} \dot{q} \\ -B(q, \dot{q}) - k(q) + \begin{bmatrix} 0 \\ \tau \end{bmatrix} \end{array} \right) \right].$$

Here, $M \in \mathbb{R}^{n \times n}$ is a positive definite inertia matrix, $B \in \mathbb{R}^n$ is a coriolis and centrifugal vector, $k \in \mathbb{R}^n$ represents the force of gravity, and $\tau \in \mathbb{R}^m$ denotes a generalized input force vector to the system. For the particular case of the two degree of freedom system of Figure 2, where $q = [\theta_1, \theta_2]^T \in \mathcal{Q}$, the detailed dynamics are presented in Appendix A. Now identify $w = Tq = [q, \dot{q}]^T \in T\mathcal{Q}$, $\tau = v$ and $\mathcal{L} = F$ in (7).

Given a submersion (i.e. a locally surjective map)

$$x = h(q), \text{ where } h : \mathcal{Q} \rightarrow \mathbb{R}^m \quad (13)$$

Identify its tangent map, $Tx = Th(Tq) = \begin{bmatrix} h(q) \\ D_q h(q) \dot{q} \end{bmatrix}$, with H in (8) and the image, Tx , with y .

The linearizing inverse function (10) is

$$L_F H^{-1}(Tq, u) = \left(D_q h \begin{bmatrix} N_{12} \\ N_{22} \end{bmatrix} \right)^{-1} \left[u - (D_q h) \dot{q} + D_q h M^{-1}(V + k) \right] \quad (14)$$

where

$$M^{-1} = \begin{bmatrix} N_{11} & N_{12} \\ N_{21} & N_{22} \end{bmatrix}, N_{11} \in \mathbb{R}^{k \times k}, N_{12} \in \mathbb{R}^{k \times m}, N_{21} \in \mathbb{R}^{m \times k}, N_{22} \in \mathbb{R}^{m \times m}.$$

Thus for Lagrangian systems, the invertibility assumption on $L_F H$ reduces to the requirement that $\left(D_q h \begin{bmatrix} N_{12} \\ N_{22} \end{bmatrix} \right)$ be full rank on Tq .

2.3 Target Trajectory and Target Dynamics

It is traditional in the underactuated robot control literature to use the linearizing feedback (10) to force y to track some reference trajectory $r_d(t)$. In the present article, we find it more useful to mimic a reference dynamical system.

Suppose we desire the output y to have the characteristics of a target dynamical system

$$\dot{y} = f(y) \quad (15)$$

Then substituting f for u in (10) we have

$$v = L_F H^{-1}(w, f(y)) = L_F H^{-1}(w, f \circ H(w)) \quad (16)$$

For example, in the sequel, we will be interested in the harmonic oscillator

$$y = Tx = \begin{bmatrix} x \\ \dot{x} \end{bmatrix}, f_\omega(Tx) = \begin{bmatrix} 0 & 1 \\ -\omega^2 & 0 \end{bmatrix} Tx \quad (17)$$

Now we consider the dynamics of the two-link brachiating robot shown in Appendix A. Motivated by the pendulum-like motion of brachiation, we choose to encode the task in terms of the target dynamical system (17). Thus, we will find it useful to introduce a submersion arising from the change of coordinates from joint space to polar coordinates on \mathbb{R}^2 ,

$$\begin{bmatrix} r \\ \theta \end{bmatrix} = \tilde{q} = \bar{g}(q) = \begin{bmatrix} l\sqrt{2(1 + \cos \theta_2)} \\ \theta_1 + \frac{1}{2}\theta_2 \end{bmatrix} \quad (18)$$

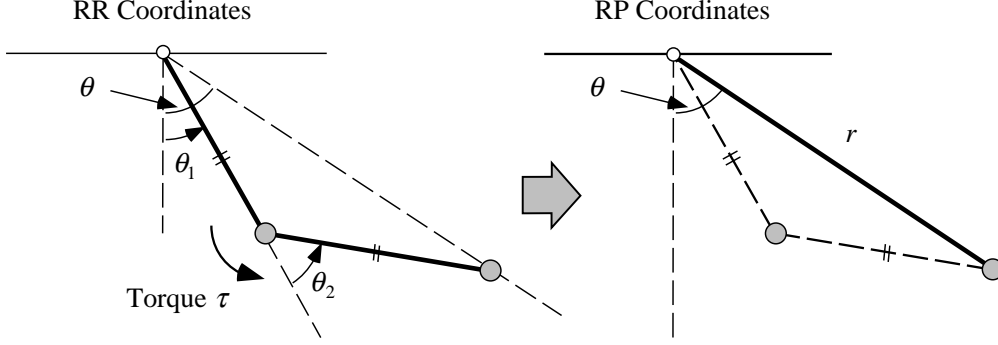


Figure 5: Change of coordinates from RR to RP. We control θ to follow the dynamics $\ddot{\theta} = -\omega^2\theta$ using target dynamics controller.

as depicted in Figure 5. Specifically, we will take the second component of (18).

$$x = h(q) := \theta = e_2^T \bar{g}(q) = \theta_1 + \frac{1}{2}\theta_2, \text{ where } e_2^T = [0, 1] \quad (19)$$

so that the application of (16) in the example of interest takes the form

$$\begin{aligned} \tau = \tau_\omega &:= L_F H^{-1}(Tq, f_\omega \circ Th(Tq)) \\ &= \left(D_q h \begin{bmatrix} n_{12} \\ n_{22} \end{bmatrix} \right)^{-1} \left[-\omega^2\theta - (D_q h)\dot{q} + D_q h M^{-1}(B + k) \right] \\ &= \frac{1}{n_{12} + \frac{1}{2}n_{22}} \left[-\omega^2(\theta_1 + \frac{1}{2}\theta_2) + (n_{11} + \frac{1}{2}n_{21})(B_1 + k_1) \right] + B_2 + k_2 \end{aligned} \quad (20)$$

where

$$M^{-1} = \begin{bmatrix} n_{11} & n_{12} \\ n_{21} & n_{22} \end{bmatrix}$$

Notice that

$$D_q h \begin{bmatrix} n_{12} \\ n_{22} \end{bmatrix} = n_{12} + \frac{1}{2}n_{22} = \frac{m_1 l^2}{2 \det(M)} \neq 0 \quad (21)$$

i.e., the invertability condition of $L_F H$ is satisfied in the particular setting of concern.

3 Ladder and Swing up Problem

We now move on to the specific problems of robot brachiation. First, we apply the target dynamics method to the ladder problem. Then, we consider the swing up problem. The target dynamics is modified to introduce a limit cycle to achieve the task. Numerical simulations are provided to suggest the effectiveness of the proposed algorithms.

3.1 Ladder problem

As we have pointed out, the ladder problem arises when an ape transfers from one branch to another and the control of arm position at the next capture represents the control task requirement. Here, we restrict our attention to brachiation on a set of evenly spaced bars at the same height. The target dynamics method is applied to the ladder problem. We show how a symmetry property of an appropriately chosen target system— (17) in the present case—can solve this problem.

3.1.1 Neutral Orbits, \mathcal{N}

This section follows closely the ideas originally developed in [11, 12]. We discuss a reverse time symmetry inherent in the brachiating robot's dynamics. First, we show that the natural dynamics of the two-link brachiating robot admit a reverse time symmetry, S . Then, we give a condition under which feedback laws result in closed loops that still admit S . Lastly, following Raibert [9], we introduce the notion of the neutral orbits of the symmetry, and show how they may be used to solve the ladder problem. In the sequel, we will denote the integral curve of a vector field f by the notation f^t .

Definition 3.1 $f : \mathcal{X} \rightarrow T\mathcal{X}$ admits a reverse time symmetry $S : \mathcal{X} \rightarrow \mathcal{X}$ if and only if $S \circ f^t = f^{-t} \circ S$.

Note that when S is linear, this definition might be equivalently stated as $S \circ f = -f \circ S$. Note that when S is linear, this definition might be equivalently stated as $S \circ f = -f \circ S$. In this paper, we are concerned specifically with the symmetry operator

$$S = \begin{bmatrix} -I_2 & 0 \\ 0 & I_2 \end{bmatrix}. \quad (22)$$

(where I_2 denotes the 2×2 identity matrix).

Now, supposing we have chosen a feedback law, $\tau(q, \dot{q})$, denote the closed loop dynamics of the robot as

$$\dot{T}q = \mathcal{L}_\tau(Tq) = \mathcal{L}(Tq, \tau(Tq)) \quad (23)$$

Say that τ “respects S ” if and only if \mathcal{L}_τ admits S .

Proposition 3.2 The closed loop dynamics \mathcal{L}_τ admits S , i.e., $S \circ \mathcal{L}_\tau(Tq) = -\mathcal{L}_\tau \circ S(Tq)$ if and only if $\tau(q, \dot{q})$ has the property $\tau(-q, \dot{q}) = -\tau(q, \dot{q})$.

Proof:

$$\begin{aligned} \mathcal{L}_\tau \circ S(Tq) &= \begin{bmatrix} \dot{q} \\ M(-q)^{-1} \left(-B(-q, \dot{q}) - k(-q) + \begin{bmatrix} 0 \\ \tau(-q, \dot{q}) \end{bmatrix} \right) \end{bmatrix} \\ &= \begin{bmatrix} \dot{q} \\ M(q)^{-1} \left(B(q, \dot{q}) + k(q) + \begin{bmatrix} 0 \\ \tau(-q, \dot{q}) \end{bmatrix} \right) \end{bmatrix} \end{aligned} \quad (24)$$

since $M(-q) = M(q)$, $B(-q, \dot{q}) = -B(q, \dot{q})$, $k(-q) = -k(q)$. On the other hand,

$$S \circ \mathcal{L}_\tau(Tq) = \begin{bmatrix} -\dot{q} \\ M(q)^{-1} \left(-B(q, \dot{q}) - k(q) + \begin{bmatrix} 0 \\ \tau(q, \dot{q}) \end{bmatrix} \right) \end{bmatrix} \quad (25)$$

From (24) and (25) we see that if $\tau(-q, \dot{q}) = -\tau(q, \dot{q})$, then $S \circ \mathcal{L}_\tau(Tq) = -\mathcal{L}_\tau \circ S(Tq)$. On the other hand, if $S \circ \mathcal{L}_\tau(Tq) = -\mathcal{L}_\tau \circ S(Tq)$, $\tau(q, \dot{q})$ has to satisfy the property $\tau(-q, \dot{q}) = -\tau(q, \dot{q})$. ■

Define the fixed points of the symmetry S to be

$$\text{Fix}S := \{Tq \in TQ \mid S(Tq) = Tq\} \quad (26)$$

In the present case, i.e., for S in (22) note that

$$\text{Fix}S = \{(q, \dot{q}) \in TQ \mid \dot{q} = 0\}$$

Define the set of “neutral orbits” to be the integral curves which go through the fixed point set,

$$\mathcal{N} := \bigcup_{t \in \mathbb{R}} \mathcal{L}^t(\text{Fix}S) \quad (27)$$

Note that a neutral orbit has a symmetry property about its fixed point—namely, if $Tq_0 \in \text{Fix}S$, then

$$S \circ \mathcal{L}^t(Tq_0) = \mathcal{L}^{-t} \circ S(Tq_0) = \mathcal{L}^{-t}(Tq_0)$$

3.1.2 The Ceiling, \mathcal{C} , and its Neutral Orbits

Define the “ceiling” to be those configurations where the hand of the robot reaches the height $y = 0$ as depicted in Figure 6.

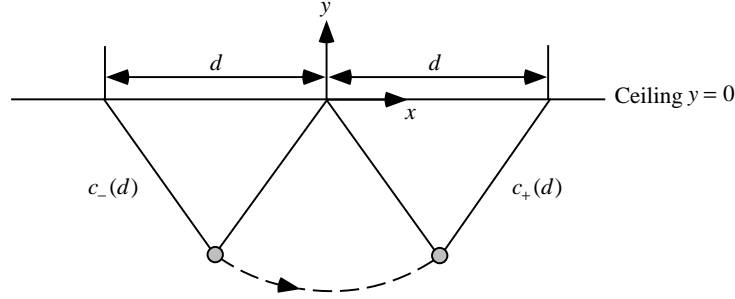


Figure 6: A ceiling configuration. The ceiling is parametrized by the distance between the grippers d . A left branch $c_-(d)$ and right branch $c_+(d)$ are defined in this manner.

$$\mathcal{C} = \{q \in Q \mid \cos \theta_1 + \cos(\theta_1 + \theta_2) = 0\}. \quad (28)$$

Note that \mathcal{C} can be parameterized by two branches,

$$\mathcal{C} = \text{Im } c_- \cup \text{Im } c_+ \quad (29)$$

of the maps, $c_{\pm} : [0, 2l] \rightarrow \mathcal{C}$,

$$c_{\pm}(d) = \begin{bmatrix} \pm \arcsin\left(\frac{d}{2l}\right) \\ \pm \left[\pi - 2 \arcsin\left(\frac{d}{2l}\right)\right] \end{bmatrix}. \quad (30)$$

In the sequel, we will be particularly interested in initial conditions of (23) originating in the zero velocity sections of the ceiling that we denote TC_0 . Now note that $S(TC_0) \subseteq TC_0$ since

$$S \begin{bmatrix} c_-(d) \\ 0 \\ 0 \end{bmatrix} = \begin{bmatrix} c_+(d) \\ 0 \\ 0 \end{bmatrix}. \quad (31)$$

Proposition 3.3 *If a feedback law, τ , respects S and if $\begin{bmatrix} c_-(d) \\ 0 \\ 0 \end{bmatrix} \in \mathcal{N} \cap TC_0$, then there can be found a time $t_N \in \mathbb{R}$ such that if $\nu = \frac{t_N}{4}$ then*

$$\mathcal{L}_{\tau}^{2\nu} \left(\begin{bmatrix} c_-(d) \\ 0 \\ 0 \end{bmatrix} \right) = \begin{bmatrix} c_+(d) \\ 0 \\ 0 \end{bmatrix} \quad (32)$$

i.e., a time at which the left branch at zero velocity in the ceiling reaches the right branch in the ceiling also at zero velocity.

Proof: By the definition of \mathcal{N} , there can be found a time $\nu \in \mathbb{R}$ at which

$$\mathcal{L}_\tau^\nu \left(\begin{bmatrix} c_-(d) \\ 0 \\ 0 \end{bmatrix} \right) := Tq^* \in \text{Fix}S \quad (33)$$

Therefore,

$$\mathcal{L}_\tau^{-\nu}(Tq^*) = \begin{bmatrix} c_-(d) \\ 0 \\ 0 \end{bmatrix}. \quad (34)$$

Applying the symmetry S , we have

$$\begin{bmatrix} c_+(d) \\ 0 \\ 0 \end{bmatrix} = S \begin{bmatrix} c_-(d) \\ 0 \\ 0 \end{bmatrix} \quad (\text{from (31)}). \quad (35)$$

But

$$S \begin{bmatrix} c_-(d) \\ 0 \\ 0 \end{bmatrix} = S \circ \mathcal{L}_\tau^{-\nu}(Tq^*) \quad (\text{from (34)}), \quad (36)$$

hence,

$$\begin{aligned} \begin{bmatrix} c_+(d) \\ 0 \\ 0 \end{bmatrix} &= S \circ \mathcal{L}_\tau^{-\nu}(Tq^*) = \mathcal{L}_\tau^\nu \circ S(Tq^*) \\ &= \mathcal{L}_\tau^\nu(Tq^*) = \mathcal{L}_\tau^\nu \circ \mathcal{L}_\tau^\nu \left(\begin{bmatrix} c_-(d) \\ 0 \\ 0 \end{bmatrix} \right) = \mathcal{L}_\tau^{2\nu} \left(\begin{bmatrix} c_-(d) \\ 0 \\ 0 \end{bmatrix} \right) \end{aligned} \quad (37)$$

■

Thus, we conclude that any feedback law, τ , which respects S , solves the ladder problem, assuming we can find a d such that $[c_-(d), 0]^T \in \mathcal{N}$. Note that finding such a ceiling point requires solving the equation

$$\Phi(d, t_N) = [I_2, 0] \mathcal{L}_\tau^\nu \left(\begin{bmatrix} c_-(d) \\ 0 \\ 0 \end{bmatrix} \right) = \begin{bmatrix} 0 \\ 0 \end{bmatrix}, \quad \text{where } \nu = \frac{t_N}{4} \quad (38)$$

for d and t_N simultaneously. Of course solving this equation is very difficult: it requires a “root finding” procedure that entails integrating the dynamics (12).

3.1.3 Application of Target Dynamics

Now we apply the notion of target dynamics described in (17). The feedback law to achieve this is given by (20):

$$\begin{aligned} \tau_\omega(Tq) &= L_F H^{-1}(Tq, f_\omega \circ Th(Tq)) \\ &= \left(D_q h \begin{bmatrix} n_{12} \\ n_{22} \end{bmatrix} \right)^{-1} \left[-\omega^2 \theta - (D_q h) \dot{q} + D_q h M^{-1}(B + k) \right] \\ &= \frac{1}{n_{12} + \frac{1}{2}n_{22}} \left[-\omega^2 \left(\theta_1 + \frac{1}{2}\theta_2 \right) + (n_{11} + \frac{1}{2}n_{21})(B_1 + k_1) \right] + B_2 + k_2 \end{aligned}$$

Notice that τ_ω respects S since $\tau_\omega(-q, \dot{q}) = -\tau_\omega(q, \dot{q})$. Notice, as well, that (17) has a very nice property relative to the difficult root finding problem (38). Namely, using this control algorithm, t_N is given by

$$t_N(\tau_\omega) = \frac{2\pi}{\omega} \quad (39)$$

because θ follows the target dynamics $\ddot{\theta} = -\omega^2\theta$. In this light, then, we need merely solve (38) for d . More formally, we seek an implicit function $d^* = \lambda^{-1}(\omega)$ such that $\Phi(\lambda^{-1}(\omega), \frac{2\pi}{\omega}) = 0$. Of course, we are more likely in practice to take an interest in tuning ω as a function of a desired d^* . Thus, we are most interested in determining

$$\omega = \lambda(d^*). \quad (40)$$

In general, we can expect no closed form expression for λ or λ^{-1} , and we resort instead to a numerical procedure for determining an estimate, $\hat{\lambda}$, as follows.

Given, d^* , take an initial guess, $\hat{\omega}_0$, using the rough approximation, $\hat{\omega}_0$ is around the range from $\sqrt{\frac{g}{l}}$ to $\sqrt{\frac{g}{2l}}$ from the simple pendulum. Then, tune $\hat{\omega}$ according to the rule:

$$\hat{\omega}_{k+1} = \hat{\omega}_k + K \left(\begin{bmatrix} 1, & 0 \end{bmatrix} \Phi(d^*, \frac{2\pi}{\hat{\omega}_k}) \right), \quad (41)$$

where K is a suitably chosen (small) gain. Iterate this procedure until

$$\left| \begin{bmatrix} 1, & 0 \end{bmatrix} \Phi(d^*, \frac{2\pi}{\hat{\omega}_k}) \right| < tolerance.$$

In practice, we have always found (41) to converge under this procedure, although we have not yet investigated the matter formally. We plot in Figure 7 a particular instance of $\hat{\lambda}$ for the case where the robot parameters are $l = 1, m_1 = 3, m_2 = 1$. We will use these parameter values throughout the sequel for the sake of comparison between this and subsequent figures.

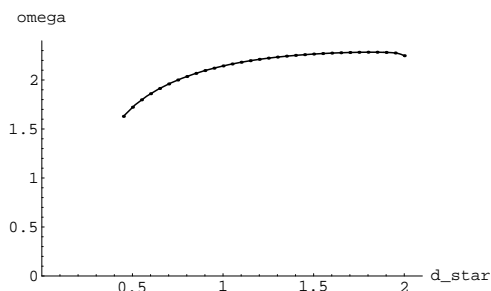


Figure 7: Numerical approximation $\omega = \hat{\lambda}(d^*)$. Target dynamics controller, τ_ω , is tuned according to this mapping, $\hat{\lambda}$, that is designed to locate neutral orbits originating in the ceiling.

3.1.4 Simulation

Consider the case $d^* = 1.4$ for this parameter set above. The initial condition of the robot is $Tq_0 = [c_-(d^*), 0]^T$. From the numerical solution depicted in Figure 7, $\omega = \hat{\lambda}(1.4) = 2.2512$. Figure 8 shows the resulting movement of the robot. The joint trajectories of θ_1, θ_2 and the trajectory of θ are shown in Figure 9. The closed loop dynamics have a neutral orbit which achieves the task.

3.2 Swing up Problem

The swing up problem entails swinging up from the suspended posture at rest and catching the next bar. In order to achieve this task it is necessary not only to pump up the energy in a suitable fashion

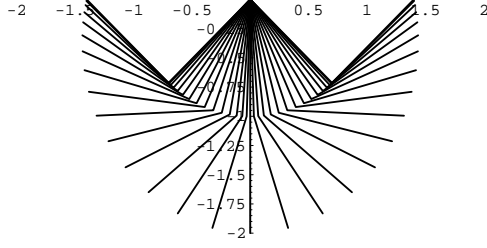


Figure 8: Movement of the robot. The symmetry properties of the neutral orbit from the ceiling solves the ladder problem.

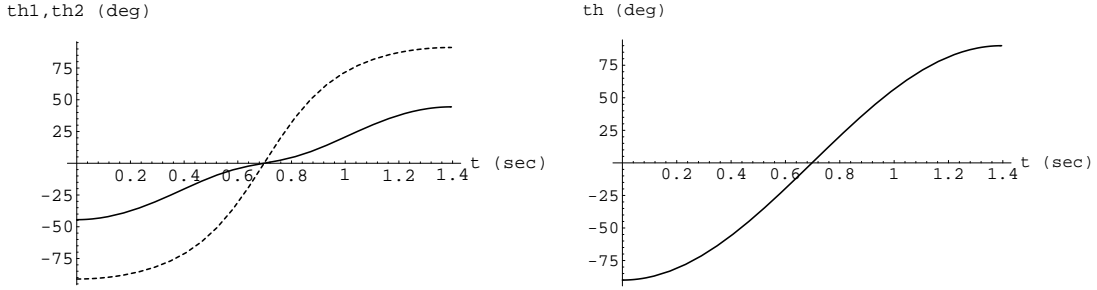


Figure 9: Joint trajectories (θ_1 : solid, θ_2 : dashed) and trajectory of θ . Note that θ follows the target dynamics $\ddot{\theta} = -\omega^2\theta$.

but also to control the arm position at the capture of the next target bar. This suggests that we need to introduce a stable limit cycle to the system with suitable magnitude and relative phase in state. The idea we present here is a simple modification of the foregoing target dynamics. We define the “pseudo energy” with respect to the target variable and add a compensation term to the target dynamics in order to introduce the desired limit cycle.

3.2.1 Modified Target Dynamics

As we have mentioned, swing up requires energy pumping in a suitable fashion. To achieve this we modify the target dynamics (17) as

$$\dot{T}x = \begin{bmatrix} 0 & 1 \\ -\omega^2 & -K_e(\bar{E} - \bar{E}^*) \end{bmatrix} Tx := f_{\bar{E}^*}(Tx) \quad (42)$$

where, $x = \theta = \theta_1 + \frac{1}{2}\theta_2$ as defined in (19)

K_e : a positive constant

$\bar{E} := \frac{1}{2}\dot{\theta}^2 + \frac{1}{2}\omega_T^2\theta^2$: “pseudo energy”

\bar{E}^* : the desired pseudo energy level

To achieve this target dynamics, the control law is formulated as

$$\begin{aligned} \tau_{\bar{E}^*} &= L_F H^{-1}(Tq, f_{\bar{E}^*} \circ Th(Tq)) \\ &= \left(D_q h \begin{bmatrix} n_{12} \\ n_{22} \end{bmatrix} \right)^{-1} \left[-\omega^2\theta - K_e(\bar{E} - \bar{E}^*) - (D_q h)\dot{q} + D_q h M^{-1}(V + k) \right] \\ &= \frac{1}{n_{12} + \frac{1}{2}n_{22}} \left[-\omega^2(\theta_1 + \frac{1}{2}\theta_2) - K_e(\bar{E} - \bar{E}^*)(\dot{\theta}_1 + \frac{1}{2}\dot{\theta}_2) + (n_{11} + \frac{1}{2}n_{21})(B_1 + k_1) \right] \\ &\quad + B_2 + k_2 \end{aligned} \quad (43)$$

Now consider the time derivative of \bar{E} along the motion

$$\dot{\bar{E}} = -K_e(\bar{E} - \bar{E}^*)\dot{\theta}^2 \quad (44)$$

If $\bar{E} > \bar{E}^*$ then the pseudo energy \bar{E} decreases, and if $\bar{E} < \bar{E}^*$ then \bar{E} increases. Therefore, \bar{E} will converge to the desired level \bar{E}^* eventually. This implies that the target dynamics with respect to θ coordinates has a stable limit cycle whose trajectory is characterized by $\frac{1}{2}\dot{\theta}^2 + \frac{1}{2}\omega^2\theta^2 = \bar{E}^*$ on the phase plane of $(\theta, \dot{\theta})$.

Although we have experienced very favorable results in numerical simulations introducing the desired limit cycle to the “target variable” using the ideas set out above, the procedure remains somewhat ad hoc. Most importantly, we need to bring the effective actuated portion of the state space, θ , to the right pseudo energy level, while simultaneously ensuring that the unactuated degree of freedom, r , coincide with the regulated length, d^* , when the trajectory enters the ceiling, TC .

As the simulation suggests, some experience is helpful in determining the proper choice of the parameters K_e, ω to give the desired motion of the robot to achieve the task. For example, large K_e seems to yield chaotic motion and small choice of K_e is preferred. Again, an elucidation of these relationships awaits a proper mathematical analysis.

3.2.2 Simulation

Suppose the next target bar is located at the distance $d^* = 1.4$. The initial condition is $q_0 = [0.01, 0]^T$ and $\dot{q}_0 = 0$. We choose the parameters in the target dynamics as $\omega = \hat{\lambda}(1.4) = 2.2512$, $K_e = 0.75$, $\bar{E}^* = \frac{1}{2}\omega^2 \left(\frac{\pi}{2}\right)^2$.

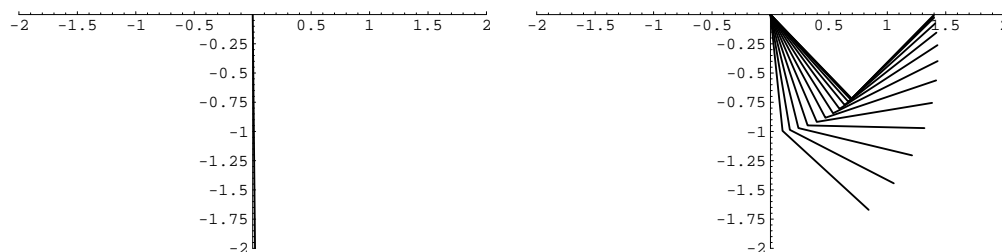


Figure 10: The initial condition at $t = 0$ (left) and movement at the capture of a bar $t = 33 \sim 33.625$ sec (right). The swing up task is achieved under the modified target dynamics.

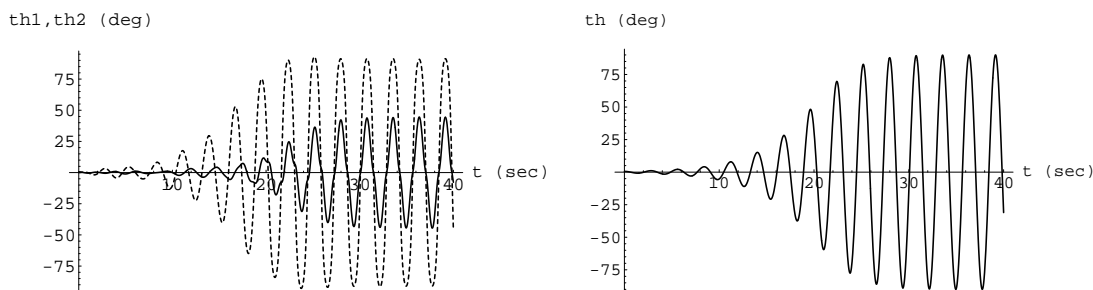


Figure 11: Joint trajectories (θ_1 : solid, θ_2 : dashed) and trajectory of θ . The desired limit cycle is achieved.

Figure 10 depicts the initial condition and the movement of the robot at the capture of a bar. Figure 11 shows the joint trajectories of θ_1, θ_2 and the trajectory of θ . These simulation results suggest that the robot can achieve the swing up and catching task via the modified target dynamics.

4 Rope problem

In this section, we consider the rope problem: brachiation along a continuum of handholds such as afforded by a branch or a rope. First, the average horizontal velocity is characterized as a result of the application of the target dynamics controller, τ_ω , introduced above. Then, we consider the regulation of horizontal velocity using this controller. An associated numerical “swing map” suggests that we indeed can achieve good local regulation of the forward velocity through the target dynamics method.

4.1 The Iterated Ladder Trajectory Induces a Horizontal Velocity

Supposing that the robot starts in the ceiling with zero velocity, then it must end in the ceiling under the target dynamics controller since θ follows the dynamics $\ddot{\theta} = -\omega^2\theta$. However, if d and ω are not “matched” as $\omega = \lambda(d)$, then the trajectory ends in the ceiling, $Tq \in TC_+$, with $\dot{\theta} = 0$ but $r \neq d$ and $\dot{r} \neq 0$. Shortly, we will present numerical evidence suggesting that when $d = d^* + \delta$ for small δ , then \dot{r} at $Tq \in TC_+$ is also small. Assuming that any such small nonzero velocity is “killed” in the ceiling, brachiation may be iterated by opening and closing the grippers at left and right ends in the appropriately coordinated manner. Namely, imagine that the robot concludes the swing by grasping firmly with its gripper the next handhold in the ceiling and thereby damps out the remaining kinetic energy. Imagine at the same instant that it releases the gripper clutching the previous handhold and thereby begins the next swing. We will call such a maneuver the Iterated Ladder Trajectory (“ILT”).

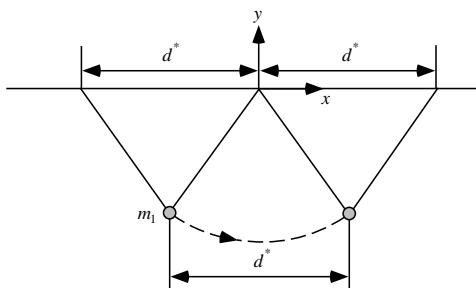


Figure 12: Progress of the robot per swing. The robot’s body proceeds d^* per swing while a gripper moves $2d^*$.

It is natural to inquire as to how quickly horizontal progress can be made along the ladder in so doing. Notice in Figure 12 that when a gripper moves a distance $2d^*$ in the course of the ladder trajectory, and if the trajectory is immediately repeated, as described above, then the body, m_1 , will also move a distance of d^* each swing, hence, its average horizontal velocity will be

$$\bar{h} = \frac{d^*\omega}{\pi} = \frac{d^*\lambda(d^*)}{\pi} := \tilde{V}_2(d^*) \quad (45)$$

according to the discussion in Section 3.1. In Figure 13, we now plot the ceiling-to-velocity map $\bar{h} = \tilde{V}_2(d^*)$ for the robot parameters $l = 1, m_1 = 3, m_2 = 1$, where \tilde{V}_2 is computed using the numerical approximation, $\hat{\lambda}$ discussed in Section 3.1.3.

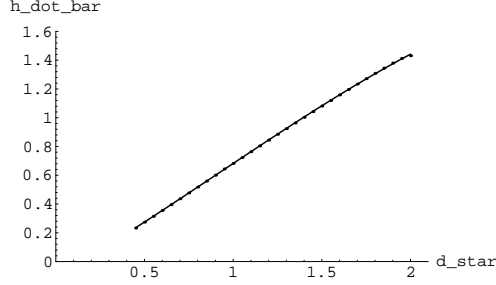


Figure 13: The ceiling-to-velocity map, \tilde{V}_2 . This mapping is inverted to obtain the desired forward velocity \bar{h}^* .

4.2 Inverting the Ceiling-to-Velocity Map

Consider now the task of obtaining the desired forward velocity \bar{h}^* of brachiation. If \tilde{V}_2 is invertible, then $d^* = \tilde{V}_2^{-1}(\bar{h}^*)$ and we can tune ω in the target dynamics as

$$\omega = \lambda \circ \tilde{V}_2^{-1}(\bar{h}^*) \quad (46)$$

to achieve a desired \bar{h}^* where λ is again the mapping (40). We have found in our numerical work that \tilde{V}_2 does, indeed, seem to be nicely invertible as suggested by the particular case of Figure 13. Further numerical exploration reveals that rewriting (45) using the kinematic relationship (3) yields a new function,

$$\hat{V}_2(\alpha_0) := \tilde{V}_2(2l \sin \alpha_0) \quad (47)$$

that is surprisingly close to the single pendulum case, $V_1(\alpha_0)$ as illustrated in Figure 14. This suggests that more careful analytical work might well suggest a simple approximation for \tilde{V}_2 as in some recent work [12] on hopping robots.

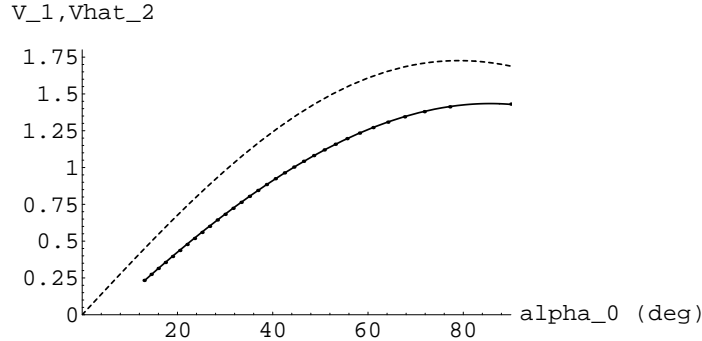


Figure 14: Velocity mapping $V_1(\alpha_0)$ (dashed) for the simple pendulum where $l_0 = 1$ and $\hat{V}_2(\alpha_0)$ (solid) for the brachiating robot with the target dynamics controller where robot parameters are $l = 1, m_1 = 3, m_2 = 1$.

4.3 Horizontal Velocity Regulation

Consider the ceiling condition with zero velocity

$$TC_{0\pm} = \left\{ \left[\begin{array}{c} c_{\pm}(d) \\ 0 \\ 0 \end{array} \right] \in TC \mid d \in [0, 2l] \right\} \quad (48)$$

Define the maps, C_{\pm} , and their inverses, C_{\pm}^{-1} , as

$$C_{\pm} : [0, 2l] \rightarrow TC_{0\pm} : d \mapsto \begin{bmatrix} c_{\pm}(d) \\ 0 \\ 0 \end{bmatrix} \quad (49)$$

$$C_{\pm}^{-1} : TC_{0\pm} \rightarrow [0, 2l] : \begin{bmatrix} c_{\pm}(d) \\ 0 \\ 0 \end{bmatrix} \mapsto d \quad (50)$$

A target dynamics controller (17) gives

$$\mathcal{L}_{\tau\omega}^{2\nu} \circ C_{-}(d) \in TC_{+}, \text{ where } \nu = \frac{\pi}{2\omega} \quad (51)$$

since θ follows the dynamics $\ddot{\theta} = -\omega^2\theta$. Now, if $\omega = \lambda(d)$, then

$$\mathcal{L}_{\tau\omega}^{2\nu} \circ C_{-}(d) = C_{+}(d) = \begin{bmatrix} c_{+}(d) \\ 0 \\ 0 \end{bmatrix} \in TC_{0+}, \text{ where } \nu = \frac{\pi}{2\omega} \quad (52)$$

because of the symmetry properties of the neutral orbits, demonstrated in Proposition 3.3.

Define a projection Π , from the ceiling's tangents into the zero velocity section,

$$\Pi : TC_{\pm} \mapsto TC_{0\pm}. \quad (53)$$

In other words, Π is a map that “kills” any velocity in the ceiling. We introduce this projection to model the ILT maneuver in cases when $\dot{r} \neq 0$ for $Tq \in TC$. We plot, \dot{r} , the approaching velocity in the right branch of the ceiling for $d \in [0, 2l]$ where $d^* = 1.26815, \omega = 2.2270$ in Figure 15.

To gain an intuitive feeling for the magnitude of “leftover energy” that must be “killed” before the next swing begins, we will compare it to the energy of the steady state swing. In the worst case, the kinetic energy in the ceiling TC_{+} resulting from the initial condition $Tq_0 = C_{-}(0.1)$ is $K(TC_{+}) = 2.09$ J. The maximum kinetic energy during a swing when $d = d^*$ is $K_{d^* \max} = 24.5$ J. The ratio $\frac{K(TC_{+})}{K_{d^* \max}} = 0.085$ seems to be acceptably small. Consider instead, more favorable range, where $d = d^* + \delta$ and $\delta = -0.3$. Now the kinetic energy killed in the ceiling is $K(TC_{+}) = 0.19$ J, and the ratio $\frac{K(TC_{+})}{K_{d^* \max}} = 7.81 \times 10^{-3}$ in this case is very small despite fairly large error (24 %) in the initial condition. This suggests that the idea of killing any approaching horizontal velocity in the ceiling may be physically reasonable. ¹

We now have from (51)

$$\Pi \circ \mathcal{L}_{\tau\omega}^{2\nu} \circ C_{-}(d) \in TC_{0+}, \text{ where } \nu = \frac{\pi}{2\omega} \quad (54)$$

hence we may define a “swing map”, σ_{ω} , as a transformation of $[0, 2l]$ into itself,

$$\sigma_{\omega}(d) := C_{+}^{-1} \circ \Pi \circ \mathcal{L}_{\tau\omega}^{2\nu} \circ C_{-}(d) : [0, 2l] \rightarrow [0, 2l] \quad (55)$$

Note that if $\omega = \omega^* = \lambda(d^*)$, then

$$\sigma_{\omega}(d^*) = d^* \quad (56)$$

that is, d^* is a fixed point of the appropriately tuned swing map.

It is now clear that the dynamics of the ILT maneuver can be modeled by the iterates of this swing map, σ_{ω} . Physically, suppose we iterate by setting the next initial condition in the ceiling to be

$$Tq_0[k+1] = C_{-} \circ \sigma_{\omega}(d[k]). \quad (57)$$

¹In Figure 15, the worst case of approaching velocity, $\dot{r} \approx 1.5$ m/s, looks fairly large, however, we are using a large model in simulation (arm length is 1m). In reality, a smaller model yields the smaller approaching velocity.

This yields a discrete dynamical system governed by the iterates of σ_ω ,

$$d[k + 1] = \sigma_\omega(d[k]).$$

Numerical evidence suggests that the iterated dynamics converges, $\lim_{k \rightarrow \infty} \sigma_\omega^{k*}(d) = d^*$, when d is in the neighborhood of d^* as depicted in Figure 16 (local asymptotic stability of the fixed point d^*). We plot the swing map calculated numerically for the case where $\bar{h} = 0.9$, $d^* = 1.26815$, $\omega = 2.2270$ and the robot parameters are $l = 1$, $m_1 = 3$, $m_2 = 1$ (see Figure 16).

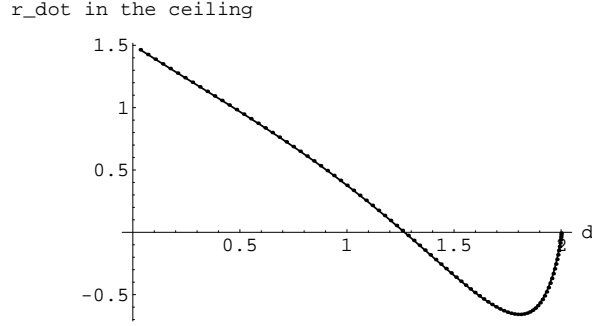


Figure 15: Approaching horizontal velocity of the robot gripper for the case $d^* = 1.26815$, $\omega^* = 2.2270$ where $\omega^* = \hat{\lambda}(d^*)$, and the robot parameters are $l = 1$, $m_1 = 3$, $m_2 = 1$. When the error in the initial condition from d^* is small, the resulting approaching velocity in the ceiling is also small.

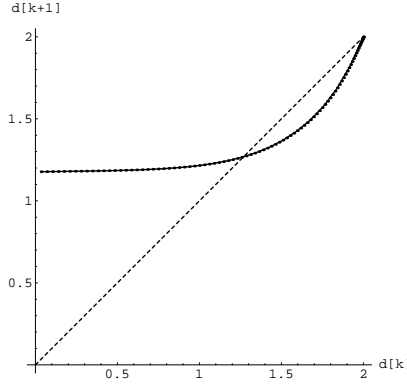


Figure 16: Swing map, σ_ω , (solid) and identity (dashed) for the case $\bar{h} = 0.9$, $d^* = 1.26815$, $\omega = 2.2270$ where $\hat{\omega}^* = \lambda(d^*)$, and the robot parameters are $l = 1$, $m_1 = 3$, $m_2 = 1$. This swing map has an attracting fixed point at d^* .

4.4 Simulation

Suppose we want to achieve the desired horizontal velocity, $\bar{h}^* = 0.9(\text{m/s})$. The parameters of the robot are $l = 1$, $m_1 = 3$, $m_2 = 1$. The procedure to obtain the numerical approximation of (46) as follows:

First, the ceiling-to-velocity map \tilde{V}_2 (45) is approximated by the third order polynomial.

$$\bar{h} = -0.04467978d^{*3} + 0.127815d^{*2} + 0.705171d^* - 0.103999 \quad (58)$$

Then, to obtain an approximation to $\tilde{V}_2^{-1}(0.9)$, (58) is solved for d^* numerically by setting $\bar{h} = 0.9$, and we get $d^* = 1.26815$. Lastly, using the numerical solution depicted in Figure 7, $\omega = \hat{\lambda}(1.2682) = 2.2270$.

First, consider ILT with the proper initial condition

$$Tq_0^* = \begin{bmatrix} c_-(d^*) \\ 0 \end{bmatrix} \quad (59)$$

which is proper in the sense $\bar{h}^* = \tilde{V}_2(d^*)$. The simulation result in this case is shown in Figure 17—a faithfully executed ILT at d^* .

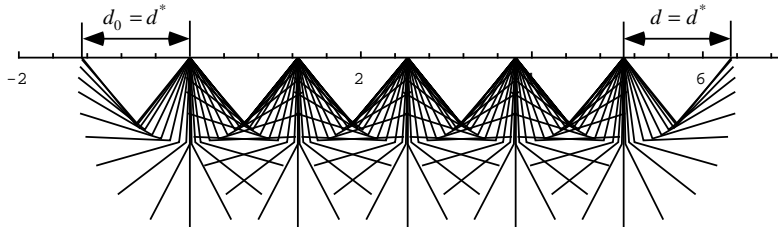


Figure 17: Brachiation along the bar with the initial condition (59). ILT locomotion at the fixed point d^* yields the desired average horizontal velocity, \bar{h}^* .

Suppose, instead, that we select $\omega = \lambda(d^*)$ but the initial d_0 is wrong. We present simulation results with the initial condition

$$Tq_0 = \begin{bmatrix} c_-(d^* + \delta) \\ 0 \end{bmatrix}, \text{ where } \delta = -0.3 \quad (60)$$

in Figure 18. As the numerical swing map of (16) suggests, we nevertheless achieve asymptotically the desired locomotion, i.e., $d \rightarrow d^*$.

With the assumption that any velocity in the ceiling is killed, the size of the domain of attraction to d^* under σ_{ω^*} is fairly large according to the numerical evidence shown in Figure 16.

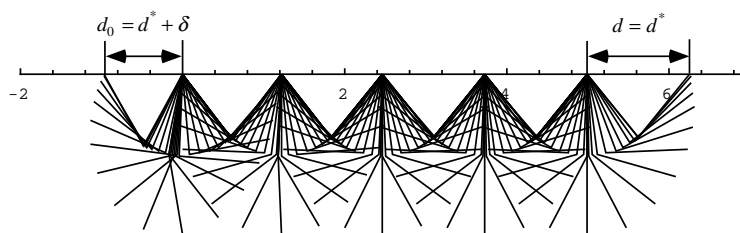


Figure 18: Brachiation along the bar with the initial condition (60). Convergence of $d \rightarrow d^*$ is illustrated as the numerical swing map (Figure 16) indicates, and this yields convergence to the desired average velocity, \bar{h}^* .

5 Conclusion

We have presented some preliminary studies of a new brachiating controller for a simplified two-link robot. The algorithm uses a target dynamics method to solve the ladder, swing up and rope problems. These tasks are encoded as the output of a target dynamical system inspired by the

pendulum-like motion of an ape’s (slow) brachiation. We provide numerical simulations suggesting the effectiveness of the proposed algorithm. However, these numerical results also show that the sensitivity to parameters, l , m_1 and m_2 may be significant. From our observation, it seems that roughly $\omega \propto \frac{1}{\sqrt{l}}$ and m_1 should be larger than m_2 . Under these circumstances, we suggest in Appendix B that the proposed algorithm is practically feasible. However a formal mathematical analysis remains to be addressed. In section 5.1 we review some of the open questions this raises and in section 5.2 we address future work.

5.1 Open Problems

These numerical simulations suggest that the proposed algorithm is effective for solving robot brachiation problems. They are far from conclusive: formal mathematical analysis will be necessary to truly understand how these ideas work. First, we need to consider the internal boundedness of the states of the closed loop system. The unactuated dynamics of our closed loop take the form of a one degree of freedom mechanical system forced by a periodic input. Such problems of parametric resonance are known to be complex. A second open problem concerns the swing map. Numerical studies suggest the local stability of the fixed point d^* but this must be verified, and the extent of the domain of attraction must be characterized.

5.2 Future Work

The controller developed in this paper requires exact model knowledge of the robot. As we have begun to contemplate experimental implementation, we would naturally prefer a robust or adaptive version. Unfortunately, there has not yet been much work on robust or adaptive control of underactuated systems.

Studies of robot brachiation using more complicated models with higher degrees of freedom will be addressed in our future work. We hope that we may find generalizable principles of brachiation through the study of this simplified two degree of freedom model.

Finally, the study of the fast brachiation—the leap problem—seems compelling. For reasons discussed in the introduction, this problem lies in the more distant future.

In the longer run, we believe that the ideas presented in this paper may have wider application to such areas of robotics as dexterous manipulation, legged locomotion and underactuated mechanisms.

Appendix

A Simplified Model of a Two-link Brachiating Robot

This section describes the two-link brachiating robot we use in this paper, shown in Figure 2. We assume each link is massless, and an actuator at the elbow and a gripper are a point mass.

Let p_1, p_2 be the position of the masses m_1, m_2 respectively. p_1, p_2 are given by

$$p_1 = \begin{bmatrix} x_1 \\ y_1 \end{bmatrix} = \begin{bmatrix} l_1 \sin \theta_1 \\ -l_1 \cos \theta_1 \end{bmatrix}, \quad p_2 = \begin{bmatrix} x_2 \\ y_2 \end{bmatrix} = \begin{bmatrix} l_1 \sin \theta_1 + l_2 \sin(\theta_1 + \theta_2) \\ -l_1 \cos \theta_1 - l_2 \cos(\theta_1 + \theta_2) \end{bmatrix}$$

The kinetic energy of the system is given by

$$K = \frac{1}{2}m_1\dot{p}_1^T\dot{p}_1 + \frac{1}{2}m_2\dot{p}_2^T\dot{p}_2$$

The potential energy of the system is given by

$$U = m_1gy_1 + m_2gy_2$$

where g is the gravity constant. Defining the Lagrangian function, $L = K - U$ and applying the Lagrangian operator yields the following equation of the motion of the system:

$$T\dot{q} = \mathcal{L}(Tq, \tau) \quad (61)$$

where

$$q = \begin{bmatrix} \theta_1 \\ \theta_2 \end{bmatrix} \in \mathcal{Q}, \quad Tq = \begin{bmatrix} q \\ \dot{q} \end{bmatrix} \in T\mathcal{Q}$$

$$\mathcal{L}(Tq, \tau) = \begin{bmatrix} \dot{q} \\ M(q)^{-1} \left(-B(q, \dot{q}) - k(q) + \begin{bmatrix} 0 \\ \tau \end{bmatrix} \right) \end{bmatrix}$$

$$M(q) = \begin{bmatrix} (m_1 + m_2)l_1^2 + m_2l_2^2 + 2l_1l_2m_2 \cos \theta_2 & m_2l_2^2 + l_1l_2m_2 \cos \theta_2 \\ m_2l_2^2 + l_1l_2m_2 \cos \theta_2 & m_2l_2^2 \end{bmatrix}$$

$$B(q, \dot{q}) = -m_2l_1l_2 \sin \theta_2 \begin{bmatrix} 2\dot{\theta}_1\dot{\theta}_2 + \dot{\theta}_2^2 \\ -\dot{\theta}_1^2 \end{bmatrix}$$

$$k(q) = \begin{bmatrix} (m_1 + m_2)gl_1 \sin \theta_1 + l_2m_2g \sin(\theta_1 + \theta_2) \\ m_2l_2g \sin(\theta_1 + \theta_2) \end{bmatrix}$$

In this paper we assume that the arm length is the same, $l_1 = l_2 = l$. Note that we have a torque input only to the second joint.

B Practical Feasibility

We consider the practical feasibility of the proposed algorithm for a typical robot configuration. Here we consider the two-link brachiating robot built by Saito [16]. The arm length is 0.5m and the total weight is 4.8kg (unfortunately the precise parameters are not known since their algorithm does not need a model of the robot). The maximum torque of the actuator is 14Nm and its rated power is 20.3W. We provide simulation results for the case where robot parameters are $l = 0.5$, $m_1 = 3$, $m_2 = 1.5$ (which seem to be reasonable for their robot configuration), and $d^* = 0.7$, $\omega = 3.07196$. Figure 19 shows the movement of the robot. The required actuator torque and power are shown in Figure 20. The required torque and power look reasonable. It must be cautioned, however, that if ω is very far out of tune, then the inverse $L_F H^{-1}$ calls for unrealistically high torque, and the resulting motion is useless.

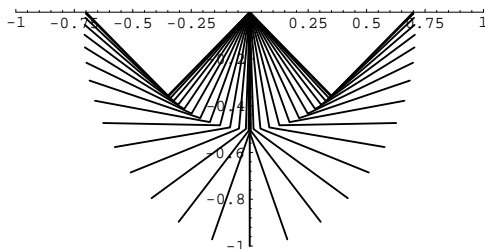


Figure 19: Movement of the robot

Acknowledgements

We would like to thank Bill Schwind and Noah Cowan at the University of Michigan for a number of illuminating discussion on this problem.

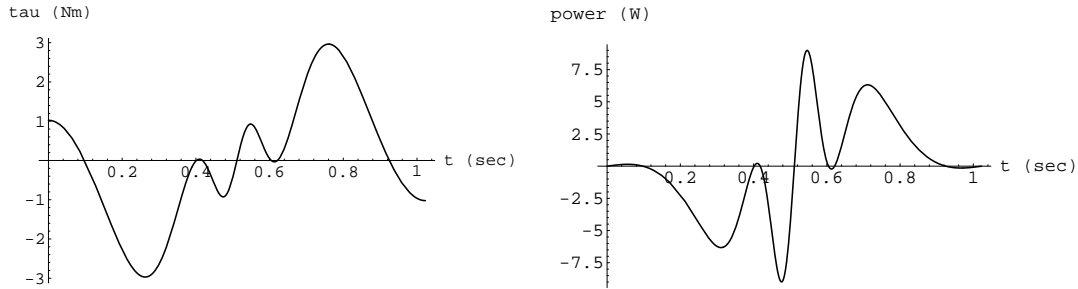


Figure 20: Required actuator torque (left) and power (right) for the case where $d^* = 0.7$, $\omega = 3.07196$ and the robot parameters are $l = 0.5$, $m_1 = 3$, $m_2 = 1.5$.

References

- [1] Andersson, R. L., *A Robot Ping-Pong Player: Experiment in Real-Time Intelligent Control*, MIT Press, 1988
- [2] Bühler, M., Koditschek, D. E. and Kindlmann, P. J., “A Family of Robot Control Strategies for Intermittent Dynamical Environments”, *IEEE Control Systems Magazine*, pp. 16-22, February, 1990
- [3] Burridge, R. R., Rizzi, A. A. and Koditschek, D. E., “Toward a Systems Theory for the Composition of Dynamically Dexterous Behaviors”, *7th International Symposium on Robotics Research*, 1995
- [4] Eimerl, S. and DeVore, I., *The Primates*, TIME-LIFE BOOKS
- [5] Koditschek, D. E., “Dynamically Dexterous Robots”, In Spong, M. W., Lewis, F. L. and Abdallah, C. T. (eds.) *Robot Control: Dynamics, Motion Planning and Analysis*, IEEE Press, pp. 487-490
- [6] Koditschek, D. E. and Bühler, M., “Analysis of a Simplified Hopping Robot”, *International Journal of Robotics Research*, Vol. 10, No. 6, pp. 587-605, December, 1991
- [7] Lynch, K. M., “Nonprehensile Robotic Manipulation: Controllability and Planning”, *Ph.D. Thesis*, Carnegie Mellon University, The Robotics Institute, March, 1996
- [8] Preuschoft, H. and Demes, B., “Biomechanics of Brachiation”, In Preuschoft, H., Chivers, D. J., Brockelman, W. Y. and Creel, N. (eds.) *The Lesser Apes*, pp. 96-118, Edinburgh University Press, 1984
- [9] Raibert, M. H., *Legged Robots that Balance*, Cambridge, MIT Press, 1986
- [10] Rizzi, A. A., Whitcomb, L. L. and Koditschek, D. E., “Distributed Real-Time Control of a Spatial Robot Juggler”, *IEEE Computer*, pp. 12-24, May, 1992
- [11] Schwind, W. J. and Koditschek, D. E., “Control the forward velocity of the simplified Planner Hopping Robot”, *Proc. IEEE International Conference on Robotics and Automation*, pp. 691-696, Nagoya, Japan, 1995
- [12] Schwind, W. J. and Koditschek, D. E., “Characterization of Monopod Equilibrium Gaits”, *Proc. IEEE International Conference on Robotics and Automation*, 1997 (in preparation for submission)

- [13] Simons, E. L., *Primate Evolution: An Introduction to Man's Place in Nature*, Macmillan
- [14] Spong, M., "Partial Feedback Linearization of Underactuated Mechanical Systems", *Proc. IEEE/RSJ International Conference on Intelligent Robots and Systems*, pp. 314-321, Munich, Germany, September, 1994
- [15] Spong, M., "The Swing Up Control Problem For The Acrobot", *IEEE Control Systems Magazine*, Vol. 15, pp. 49-55, February, 1995
- [16] Saito, F. , Fukuda, T. and Arai, F., "Swing and Locomotion Control for a Two-Link Brachiation Robot", *IEEE Control Systems Magazine*, Vol. 12, pp. 5-12, February, 1994
- [17] Saito, F., "Motion Control of the Brachiation Type of Mobile Robot", *Ph.D Thesis*, Nagoya University, Nagoya, Japan, March, 1995 (in Japanese)